Detection and Decoding in Large-Scale MIMO Systems: A Non-Binary Belief Propagation Approach

T. Lakshmi Narasimhan and A.Chockalingam
Department of ECE, Indian Institute of Science, Bangalore 560012

***Abstract*—In this paper, we propose a non-binary belief propagation approach (NB-BP) for detection of M-ary modulation symbols and decoding of q-ary LDPC codes in large-scale multiuser MIMO systems. We first propose a message passing based symbol detection algorithm which computes vector messages using a scalar Gaussian approximation of interference, which results in a total complexity of just $O(KN\sqrt{M})$, where K is the number of uplink users and N is the number of base station (BS) antennas. We then design optimized q-ary LDPC codes by matching the EXIT charts of the proposed detector and the LDPC decoder. Simulation results show that the proposed NB-BP detection-decoding approach using the optimized LDPC codes achieve significantly better performance (by about 1 dB to 7 dB at 10^{-5} coded BER for various system loading factors with number of users ranging from 16 to 128 and number of BS antennas fixed at 128) compared to using linear detectors and off-the-shelf q-ary irregular LDPC codes.**

I. Introduction

Wireless communication systems using multiple-input multiple-output (MIMO) configurations with a large number of antennas have recently attracted a lot of research attention [1], [2]. These systems can achieve high spectral and power efficiencies. An emerging architecture for large-scale multiuser MIMO communications is one where each base station (BS) is equipped with a large number of antennas and the user terminals are equipped with one antenna each. A key requirement on the uplink (user terminal to BS link) in such large-scale MIMO systems is to achieve reduced detection and decoding complexities at the BS receiver to enable practical implementation, while maintaining good performance. When the number of BS antennas is much larger than the number of uplink users (i.e., low system loading factors), linear detectors like the minimum mean square error (MMSE) detector are good in terms of both complexity and performance [3].

Belief propagation (BP) on graphs is a promising low-complexity high-performance approach for signal processing in large dimensions. Decoding of turbo codes and low density parity check (LDPC) codes, and equalization/detection [4]-[7] are popular examples of the use of BP in communications. In [6], a MIMO detection algorithm for binary modulation, based on approximate message passing on a factor graph is presented. We refer to this algorithm in [6] as *binary-BP* (B-BP) algorithm. The total complexity of the B-BP algorithm is very low (quadratic in the number of dimensions) because of its Gaussian approximation of interference. Though the performance of the B-BP algorithm in large dimensions is very good for binary modulation (BPSK), its performance in higher-order QAM is rather poor (we will see this in results/discussions in Sec. III). The BP algorithm in [7] uses a different approach. It obtains a tree that approximates the fully-connected MIMO graph and performs message passing on this tree. The performance of this detection algorithm for higher-order QAM is also far from optimal.

The non-binary BP approach achieves good performance at low complexities for q-ary LDPC codes [8]. In this paper, we propose a *non-binary BP (NB-BP) approach for both detection as well as decoding* which achieves very good complexity and performance in large-scale multiuser MIMO systems. Our new contributions in this paper can be summarized as follows:

- First, we propose a NB-BP based detection algorithm for M-ary modulation, where (i) the messages passed between nodes are constructed as vector messages, and (ii) the interference is approximated as a scalar Gaussian random variable. While the scalar approximation contributes to achieving very low complexity (*lower than MMSE complexity*), the vector nature of the messages contribute to achieving close to optimal performance in large dimensions.
- Next, through the EXIT curve matching technique, we obtain q-ary LDPC codes that are optimized for the proposed NB-BP detector and the LDPC decoder. These optimized irregular q-ary LDPC codes with NB-BP detection outperform off-the-shelf irregular q-ary LDPC codes with MMSE detection, by 1 dB to 7 dB at 10^{-5} coded BER for various system loading factors; the number of users is varied from 16 to 128 and the number of BS antennas is fixed at 128.

To our knowledge, non-binary BP for detection of M-ary modulation and q-ary LDPC code optimization for large-scale multiuser MIMO systems have not been reported so far.

II. System Model

Consider a large-scale multiuser MIMO system where K uplink users, each transmitting with a single antenna, communicate with a BS having a large number of receive antennas. Let N denote the number of BS antennas; N is in the range of tens to hundreds. The ratio $\alpha = K/N$ is the system loading factor. This system model is illustrated in Fig. 1. Each user uses an LDPC code over GF(q) and M-QAM modulation. Each user encodes a sequence of $k\beta$ information bits to a sequence of n coded symbols using

978-1-4799-4482-8/14/$31.00 ©2014 IEEE

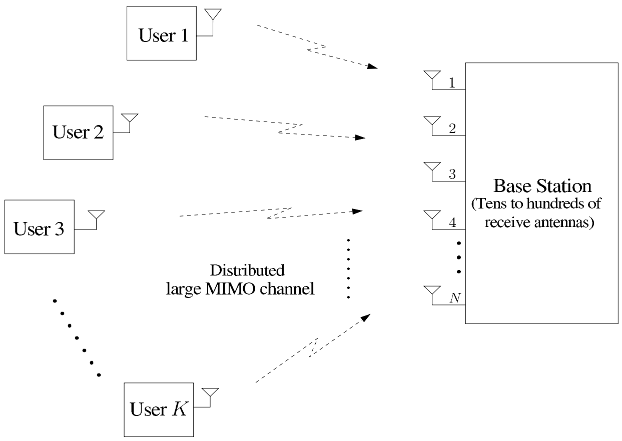

Fig. 1. An illustration of the uplink multiuser-user MIMO system with K transmitting users and N receiving antennas at the base station.

a q-ary LDPC code with parity check matrix $\mathbf{F}$ and code rate $R = \frac{k}{n}$, where $\beta = \log_2 q$. These coded symbols are then M-QAM modulated and transmitted. Assume $M = q = 2^{2i}$, where i is any positive integer. The transmission of one LDPC code block requires n channel uses. Let $\mathbf{H}_c^{(t)} \in \mathbb{C}^{N\times K}$ denote the channel gain matrix in the tth channel use and h_{ij}^c denote the complex channel gain from the jth user to the ith BS antenna. The channel gains h_{ij}^c's are assumed to be independent Gaussian with zero mean and variance σ_j^2, such that $\sum_j \sigma_j^2 = K$. Each σ_j^2 models the imbalance in the received power from user j due to path loss etc., and $\sigma_j^2 = 1$ corresponds to the case of perfect power control. Let $\mathbf{x}_c^{(t)}$ denote the modulated symbol vector transmitted in the tth channel use, where the jth element of $\mathbf{x}_c^{(t)}$ denotes the modulation symbol transmitted by the jth user. Assuming perfect synchronization, the received vector at the BS in the tth channel use, $\mathbf{y}_c^{(t)}$, is given by

$$\mathbf{y}_c^{(t)} = \mathbf{H}_c^{(t)}\mathbf{x}_c^{(t)} + \mathbf{w}_c^{(t)}, \quad (1)$$

where $\mathbf{w}_c^{(t)}$ is the noise vector whose entries are modeled as i.i.d. $\mathcal{CN}(0,\sigma^2)$. Dropping the channel use index for convenience, (1) can be written in the real domain as

$$\mathbf{y} = \mathbf{H}\mathbf{x} + \mathbf{w}, \quad (2)$$

where $\mathbf{y} \triangleq \begin{bmatrix} \Re(\mathbf{y}_c) \\ \Im(\mathbf{y}_c) \end{bmatrix}$, $\mathbf{H} \triangleq \begin{bmatrix} \Re(\mathbf{H}_c) & -\Im(\mathbf{H}_c) \\ \Im(\mathbf{H}_c) & \Re(\mathbf{H}_c) \end{bmatrix}$, $\mathbf{x} \triangleq \begin{bmatrix} \Re(\mathbf{x}_c) \\ \Im(\mathbf{x}_c) \end{bmatrix}$, $\mathbf{w} \triangleq \begin{bmatrix} \Re(\mathbf{w}_c) \\ \Im(\mathbf{w}_c) \end{bmatrix}$, and $\Re(.)$ and $\Im(.)$ denote the real and imaginary parts, respectively. Note that for M-QAM modulation, the elements of $\mathbf{x}$ come from the underlying PAM alphabet $\mathbb{A} = \{\pm 1, \pm 3, \cdots, \pm\sqrt{M}-1\}$. The BS observes $\mathbf{y}$ and performs detection and decoding.

III. Non-Binary BP for Detection

In this section, we propose a NB-BP scheme for the detection of M-QAM symbols suited well for large-scale MIMO systems. A key component of the scheme is the proposed construction of vector messages over a factor graph using a scalar Gaussian approximation of interference. While the scalar approximation contributes to achieving very low complexity, the vector nature of the messages contributes to achieving very good performance.

We model the system as a factor graph with N observation nodes and K variable nodes (see Fig. 2), and perform an approximate marginalization of the symbol probabilities over this graph. The ith element in the received vector $\mathbf{y}$ can be written as

$$y_i = h_{ij}x_j + z_{ij}, \quad i = 1,\cdots,2N, \ j = 1,\cdots,2K, \quad (3)$$

where $z_{ij} \triangleq \sum_{l=1,l\neq j}^{2K} h_{il}x_l + w_i$ is the interference-plus-noise term, x_j is the jth element in $\mathbf{x}$, h_{ij} is the (i,j)th element in $\mathbf{H}$, and w_i is the ith element in $\mathbf{w}$. As in [6], we approximate the scalar term z_{ij} as Gaussian r.v.[1] with mean (μ_{ij}) and variance (σ_{ij}^2), given by

$$\mu_{ij} = \sum_{l=1,l\neq j}^{2K} h_{il}\mathbb{E}(x_l), \quad \sigma_{ij}^2 = \sum_{l=1,l\neq j}^{2K} h_{il}^2 \,\mathrm{Var}(x_l) + \sigma^2. \quad (4)$$

Construction of vector messages: Let $\mathbf{a}_{ij}$ denote the message passed from the ith observation node to the jth variable node, and $\mathbf{v}_{ji}$ denote the message passed from the jth variable node to ith observation node (see Fig. 2). $\mathbf{a}_{ij}$ and $\mathbf{v}_{ji}$ are vectors of size $\sqrt{M}\times 1$, and they are constructed to be functions of the approximate likelihood and posterior probabilities. Using the Gaussian approximation made above, the likelihood and the posterior probabilities can be approximated as

$$\Pr(y_i|\mathbf{H}, x_j = s) \approx \frac{1}{\sigma_{ij}\sqrt{2\pi}}\exp\Big(\frac{-(y_i-\mu_{ij}-h_{ij}s)^2}{2\sigma_{ij}^2}\Big), \quad (5)$$

where $s \in \mathbb{A}$, and

$$\begin{aligned}\Pr(x_j = s|\mathbf{y},\mathbf{H}) &\propto \prod_{i=1}^{2N}\Pr(y_i|\mathbf{H}, x_j = s) \\ &\approx \prod_{i=1}^{2N}\frac{\exp\Big(\frac{-(y_i-\mu_{ij}-h_{ij}s)^2}{2\sigma_{ij}^2}\Big)}{\sigma_{ij}}, \quad (6)\end{aligned}$$

respectively. With these approximations, the messages are defined as

$$a_{ij}(s) = \frac{1}{\sigma_{ij}\sqrt{2\pi}}\exp\Big(\frac{-(y_i-\mu_{ij}-h_{ij}s)^2}{2\sigma_{ij}^2}\Big), \quad (7)$$

$$v_{ji}(s) = \prod_{l=1,l\neq i}^{2N} a_{lj}(s). \quad (8)$$

where $a_{ij}(s)$ and $v_{ij}(s)$ are the elements of $\mathbf{a}_{ij}$ and $\mathbf{v}_{ij}$, respectively, corresponding to the symbol s. The mean and variance at the ith observation node are computed as

[1] *Remark:* Although a similar scalar approximation of interference is used in [6], here the proposed formulation of messages as vectors achieves significantly improved M-QAM detection performance compared to the scalar messages based BP in [6].

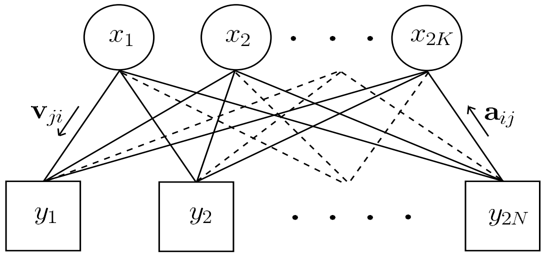

Fig. 2. The factor graph and vector messages.

$$\mu_{ij} = \sum_{l=1, l\neq j}^{2K} h_{il}\mathbf{s}^T\mathbf{v}_{li}, \tag{9}$$

$$\sigma_{ij}^2 = \sum_{l=1, l\neq j}^{2K} h_{il}^2 \left((\mathbf{s}\odot\mathbf{s})^T\mathbf{v}_{li} - (\mathbf{s}^T\mathbf{v}_{li})^2 \right) + \sigma^2. \tag{10}$$

where $\mathbf{s}$ is the vector of all elements in $\mathbb{A}$ (e.g., for $M = 16$, $\mathbf{s} = [-3\ -1\ +1\ +3]^T$), and $\odot$ denotes the Hadamard product of vectors. *Message passing:*

Step 1) Initialize the posterior probability values $v_{ji}(s)$'s as $1/\sqrt{M}$.
Step 2) Compute $\mathbf{a}_{ij}$ messages using (9), (10), and (7).
Step 3) Compute $\mathbf{v}_{ji}$ messages using (8). This forms one iteration of the algorithm.
Repeat Steps 2) and 3) for a certain number of iterations. Damping on $\mathbf{v}_{ji}$ messages can be done in the mth iteration using a damping factor δ as

$$\mathbf{v}_{ji}^{(m)} = (1-\delta)\mathbf{v}_{ji}^{(m)} + \delta\mathbf{v}_{ji}^{(m-1)}, \quad \delta \in [0,1). \tag{11}$$

After a given number of iterations, the final symbol probabilities are computed as

$$P_{x_j}(s) \ \stackrel{\triangle}{=}\ \Pr(x_j = s) \ \propto\ \prod_{l=1}^{2N} a_{lj}(s). \tag{12}$$

A listing of the proposed NB-BP algorithm is listed in **Algorithm 1**. The $P_{x_j}(s)$ values $\forall s, j$ are fed as soft inputs to the q-ary LDPC decoder. In uncoded systems, hard bit decisions are made on the bit probability values computed as

$$\Pr(b_j^p = 1) = \sum_{\forall s\in\mathbb{A}:\ p\text{th bit in } s \text{ is } 1} P_{x_j}(s), \tag{13}$$

where b_j^p is the pth bit in the jth user's symbol.

Complexity: From (8), (9) and (10), the total complexity of the NB-BP scheme proposed above is $O(KN\sqrt{M})$. This is because the summations in (9), (10) can be computed by summing over all node indices once and subtracting from it the term to be excluded at each node. *Note that the $O(KN\sqrt{M})$ complexity of the proposed scheme is much less compared to the MMSE detector complexity of $O(KN^2)$. This is because the MMSE detector needs a matrix inversion, whereas the proposed NB-BP scheme does not need a matrix inversion. More interestingly, as discussed next, even with this less than MMSE complexity, the proposed NB-BP scheme performs increasingly closer to optimal performance in large-scale MIMO systems.*

Input: $\mathbf{y}$, $\mathbf{H}$, σ^2
Initialize: $v_{ji}^{(0)}(s) \leftarrow 1/\sqrt{M}$, $\forall i, j, s$
for $m = 1 \rightarrow Number\_of\_iterations$ **do**
  for $i = 1 \rightarrow 2N$ **do**
    $\mu_i \leftarrow \sum_{l=1}^{2K} h_{il}\mathbf{s}^T\mathbf{v}_{li}^{(m-1)}$
    $\sigma_i^2 \leftarrow \sum_{l=1}^{2K} h_{il}^2 \left((\mathbf{s}\odot\mathbf{s})^T\mathbf{v}_{li}^{(m-1)} - (\mathbf{s}^T\mathbf{v}_{li}^{(m-1)})^2 \right) + \sigma^2$
    for $j = 1 \rightarrow 2K$ **do**
      $\mu_{ij} \leftarrow \mu_i - h_{ij}\mathbf{s}^T\mathbf{v}_{ji}^{(m-1)}$
      $\sigma_{ij}^2 \leftarrow \sigma_i^2 - h_{ij}^2 \left((\mathbf{s}\odot\mathbf{s})^T\mathbf{v}_{ji}^{(m-1)} - (\mathbf{s}^T\mathbf{v}_{ji}^{(m-1)})^2 \right)$
      foreach $s \in \mathbb{A}$ **do**
        $a_{ij}(s) \leftarrow \frac{1}{\sigma_{ij}\sqrt{2\pi}} \exp\left(\frac{-(y_i - \mu_{ij} - h_{ij}s)^2}{2\sigma_{ij}^2} \right)$
      end
    end
  end
  for $j = 1 \rightarrow 2K$ **do**
    foreach $s \in \mathbb{A}$ **do**
      $v_j^{(m)}(s) \leftarrow \prod_{l=1}^{2N} a_{lj}(s)$
    end
    for $i = 1 \rightarrow 2N$ **do**
      foreach $s \in \mathbb{A}$ **do**
        $v_{ji}^{(m)}(s) \leftarrow v_j(s)/a_{ij}(s)$
      end
      $\mathbf{v}_{ji}^{(m)} = (1-\delta)\mathbf{v}_{ji}^{(m)} + \delta\mathbf{v}_{ji}^{(m-1)}$
    end
  end
end
Output: $P_{x_j}(s) \leftarrow \frac{1}{Z}\prod_{l=1}^{2N} a_{lj}(s)$, Z is normalizing constant.

Algorithm 1: The proposed NB-BP detection algorithm.

BER Performance: Figure 3 shows the uncoded BER performance of the proposed NB-BP detector for 16-QAM in multiuser MIMO with $N = 32, 64, 128, 256$, $\alpha = 1$, and $\sigma_j = 1$. The performance of the B-BP detector in [6], MMSE detector, MF detector, and unfaded SISO AWGN performance are also plotted for comparison. For using the B-BP scheme in [6] for M-QAM detection, each M-QAM symbol is written in the form of linear combination of the constituent q bits and the equivalent system model is written as $\mathbf{y} = \mathbf{H}(\mathbf{I}_K \otimes \mathbf{m})\mathbf{x}_b + \mathbf{w}$, where $\mathbf{m} = [2^0\ 2^1\ \cdots\ 2^{\frac{\beta}{2}-1}]$, $\mathbf{x}_b \in \{\pm 1\}^{K\beta}$ is the vector of information bits, and the B-BP algorithm is run on the equivalent bit-level system model with the resulting complexity being the same as that of NB-BP. In the simulations, the number of BP iterations used is 40 and the damping factor used is $\delta = 0.2$. From Fig. 3, we observe that the NB-BP detector performs considerably better than the MMSE and MF detectors. In large dimensions (e.g., $N = 256$), the NB-BP detector performance gets very close to SISO-AWGN performance. Also, the NB-BP scheme significantly outperforms the B-BP scheme (e.g., for $N = 256$, NB-BP performs better than B-BP by about 8 dB at 10^{-3} BER). This is because, with M-QAM, the assumption that the elements of $\mathbf{x}_b$ in B-BP are independent is not true, and this results in a degraded performance in B-BP when applied to M-QAM.

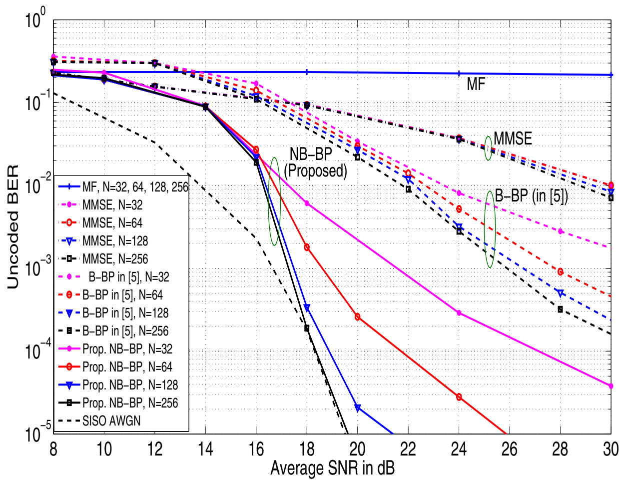

Fig. 3. Comparison of uncoded BER performance of the proposed NB-BP scheme with those of B-BP in [6], MMSE and MF detectors for $N = 32, 64, 128, 256$, $\alpha = 1$, and 16-QAM.

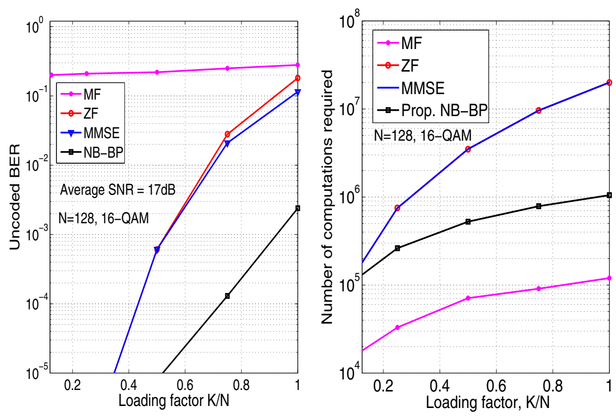

(a) Performance

(b) Complexity

Fig. 4. Comparison of uncoded BER performance and complexity of the proposed NB-BP scheme with those of linear detectors (MMSE, ZF, MF) as a function of loading factor α, with $N = 128$ and 16-QAM.

Next, in Figs. 4(a) and 4(b), we show performance and complexity comparison of NB-BP with MMSE, ZF, and MF detectors for varying loading factors at 17 dB SNR, $N = 128$ and 16-QAM. As mentioned earlier, we can see that the NB-BP scheme achieves better performance than ZF and MMSE detectors at lesser complexity than these detectors across various loading factors, α.

IV. Optimized LDPC Code Design for NB-BP Detector-Decoder

In this section, we compute the EXIT chart of the NB-BP detector combined with the q-ary LDPC decoder, and obtain the optimal degree profile distribution of the q-ary LDPC code. The q-ary LDPC codewords are decoded by a message passing algorithm over a bipartite graph made of n variable nodes and k check nodes. A detailed description of non-binary LDPC decoding algorithm can be found in [8],[12]. As in [11], we formulate an integrated graph consisting of three sets of nodes, namely, variable nodes set, observation nodes set, and check nodes set. There are nN observation nodes corresponding to the received vectors, nK variable nodes corresponding to the transmitted coded symbol vectors, and $K(n-k)$ check nodes corresponding to the check equations of the LDPC code. Combining the NB-BP detector proposed in the previous section and the non-binary LDPC decoder, a joint message passing scheme is formulated for joint detection-decoding.

EXIT analysis: We use the EXIT chart analysis for analyzing the behavior of joint detector-decoder. If I_A is the average mutual information between the coded symbols and input a priori information, and I_E is the average mutual information between the coded symbols and the extrinsic output, then the EXIT function is $f(I_A) = I_E$. To obtain the EXIT characteristics of the joint detector-decoder, we first obtain the EXIT curves of the NB-BP detector and combine it with that of the LDPC decoder.

Let $I_{E,nbbp}$ and $I_{A,nbbp}$ denote the I_E and I_A, respectively, for the NB-BP detector. Then the EXIT function is $I_{E,nbbp} = f(\gamma, K, N, I_{A,nbbp})$, where γ is the average received SNR. Since an analytical evaluation of this function is difficult, we compute it through Monte Carlo simulations [10]. If d_v and d_c denote the variable node and check node degrees, respectively, of the LDPC code, then the EXIT function [12], [10] of the LDPC variable nodes set is given by $I_{E,V} = J\left(\sqrt{(d_v-1)(J^{-1}(I_{A,V}))^2 + c\gamma}\right)$, and the EXIT function of the LDPC check nodes set is given by $I_{E,C} = 1 - J\left(J^{-1}(1-I_{A,C})\sqrt{(d_c-1)}\right)$, where c is a constant dependent on q and $J(.)$ is as defined in [10].

We formulate the EXIT function of the combination of the NB-BP detector and the variable nodes set of the q-ary LDPC decoder as

$$I_{E,JV}(\gamma, d_v, I_{A,JV}, I_{E,nbbp}) = J\left(\sqrt{(d_v-1)(J^{-1}(I_{A,JV}))^2 + (J^{-1}(I_{E,nbbp}))^2}\right), \quad (14)$$

where $I_{E,JV}$ and $I_{A,JV}$ are the I_E and I_A, respectively, for the combined variable nodes set. We match this EXIT curve with that of the check nodes set, such that the EXIT curve of the check nodes set lie below the EXIT curve of the combined variable nodes set.

Optimized LDPC code design procedure: To approach the capacity of the channel, the EXIT curves of the check nodes set and the variable nodes set should be matched. This matching is done by obtaining an appropriate degree distribution of the variable nodes and the check nodes, thereby designing irregular LDPC codes for a specific channel and receiver. The design methodology we adopt is described in detail in [13]. We use the method described in [9] to optimize the non-zero entries of the parity check matrix. By this method, the combination of the non-zero entries of a row of the parity check matrix that maximize the average entropy of the syndrome vector is chosen to be the entries of the row of our parity check matrix, $\mathbf{F}$. We obtained optimized non-binary irregular LDPC codes using the design procedure described above, and the obtained codes for different system settings and loading factors are given in Table I.

Parameters	$N = 128$, $\alpha = 1$	$N = 128$, $\alpha = 0.5$	$N = 128$, $\alpha = 0.25$
(d_v, p_v)	(2, 0.4768), (6, 0.0104), (8, 0.3174), (12, 0.1817), (16, 0.0024), (20, 0.0113)	(2, 0.6246), (8, 0.168) (16, 0.1853), (20, 0.0221)	(2, 0.3557), (3, 0.6018), (8, 0.0067), (12, 0.0358)
(d_c, p_c)	(6, 0.5206), (10, 0.1973), (18, 0.1517), (32, 0.1304)	(8, 0.5649), (16, 0.1755), (18, 0.2596)	(5, 0.7287), (8, 0.1793), (10, 0.0922)

TABLE I. DEGREE PROFILES OF OPTIMIZED RATE-1/2 16-ARY LDPC CODES FOR DIFFERENT LARGE MULTIUSER MIMO CONFIGURATIONS. p_v, p_c: FRACTION OF VARIABLE NODES WITH DEGREE d_v AND CHECK NODES WITH DEGREE d_c.

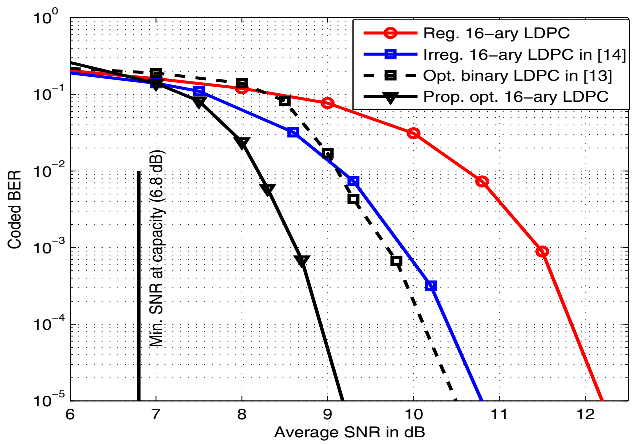

Fig. 5. Performance comparison of the proposed irregular non-binary LDPC codes with other LDPC codes for $n = 1000$ coded symbols, 16-QAM and $N = K = 64$, at a spectral efficiency of 128 bits/s/Hz.

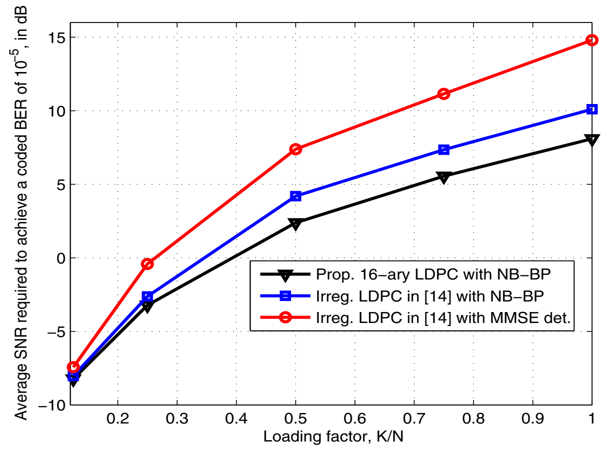

Fig. 6. Performance comparison of the proposed irregular non-binary LDPC codes with other LDPC codes for $n = 1000$ coded symbols and 16-QAM. $N = 128$ for different loading factors.

Coded BER performance: We evaluated the coded BER performance of the proposed non-binary LDPC codes and compared with those of other LDPC codes, namely, (i) random non-binary 'regular' LDPC code, (ii) non-binary irregular LDPC code in [14], and (iii) optimized 'binary' irregular LDPC code in [13]. Figure 5 shows the simulated coded BER performance of the proposed rate-1/2 non-binary LDPC code with $n = 1000$ coded symbols using NB-BP detection and decoding in a system with $N = 64$, $\alpha = 1$, and 16-QAM. It can be seen that the proposed code significantly outperforms other codes; e.g., by about 1.2 to 3 dB at 10^{-5} coded BER. The better performance of the proposed code is because of the matching of EXIT charts of the combined NB-BP detector and non-binary LDPC decoder. Also, the proposed code's performance is just about 2.3 dB away from capacity. Figure 6 shows the average SNR required to achieve a coded BER of 10^{-5} by the proposed rate-1/2 non-binary LDPC codes with NB-BP detection as a function of loading factor for $N = 128$, $n = 1000$ coded symbols, and 16-QAM. It can be seen that this performance is better than the performance achieved by the non-binary LDPC code in [14] with MMSE detection and NB-BP detection, by 1 dB to 7 dB for various system loading factors.

V. Conclusions

We proposed a promising non-binary BP algorithm for M-QAM signal detection in large-scale MIMO systems. An interesting feature of the proposed algorithm from an implementation view point is that it achieves close to optimum performance in large-scale MIMO systems with less than MMSE complexity. It also enabled the design of good LDPC codes matched to large MIMO channels.

References

[1] A. Chockalingam and B. Sundar Rajan, *Large MIMO Systems*, Cambridge Univ. Press, Feb. 2014.

[2] F. Rusek, D. Persson, B. K. Lau, E. G. Larsson, T. L. Marzetta, O. Edfors, and F. Tufvesson, "Scaling up MIMO: opportunities and challenges with very large arrays," *IEEE Signal Process. Mag.*, vol. 30, no. 1, pp. 40-60, Jan. 2013.

[3] J. Hoydis, S. ten Brink, and M. Debbah, "Massive MIMO in the UL/DL of cellular networks: how many antennas do we need?" *IEEE J. Sel. Areas in Commun.*, vol. 31, no. 2, pp. 160-171, Feb. 2013.

[4] R. J. McEliece, D. J. C. MacKay, and J-F. Cheng, "Turbo decoding as an instance of Pearls "belief propagation" algorithm," *IEEE J. Sel. Areas in Commun.*, vol. 16, no. 2, pp. 140-152, Feb. 1998.

[5] B. M. Kurkoski, P. H. Siegel, and J. K. Wolf, "Joint message-passing decoding of LDPC codes and partial-response channels," *IEEE Trans. Inform. Theory*, vol. 48, no. 6, pp. 1410-1422, Jun. 2002.

[6] P. Som, T. Datta, N. Srinidhi, A. Chockalingam, and B. S. Rajan, "Low-complexity detection in large-dimension MIMO-ISI channels using graphical Models," *IEEE J. Sel. Topics in Signal Process.*, vol. 5, no. 8, pp. 1497-1511, Dec. 2011.

[7] J. Goldberger and A. Leshem, "MIMO detection for high-order QAM based on a Gaussian tree approximation," *IEEE Trans. Inform. Theory*, vol. 57. no. 8, pp. 4973-4982, Aug. 2011.

[8] M. Davey and D. MacKay, "Low density parity check codes over GF(q)," *IEEE Commun. Letters*, vol. 2, no. 6, pp. 165-167, Jun. 1998.

[9] D. MacKay, "Optimizing sparse graph codes over GF(q)," online: http://www.inference.phy.cam.ac.uk/mackay/CodesGallager.html

[10] S. ten Brink, G. Kramer, and A. Ashikhmin, "Design of low-density parity-check codes for modulation and detection," *IEEE Trans. Commun.*, vol. 52, no. 4, pp. 670-678, Apr. 2004.

[11] T. L. Narasimhan, A. Chockalingam, and B. S. Rajan, "Factor graph based joint detection/decoding for LDPC coded large MIMO systems," *Proc. IEEE VTC'2012-Spring*, May 2012.

[12] A. Bennatan and D. Burshtein. "Design and analysis of nonbinary LDPC codes for arbitrary discrete-memoryless channels," *IEEE Trans. Inform. Theory*, vol. 52, no.2, pp. 549-583, Feb. 2006.

[13] T. L. Narasimhan and A. Chockalingam, "EXIT chart based design of irregular LDPC codes for large MIMO systems," *IEEE Commun. Letters*, vol. 17, no. 1, pp. 115-118, Jan. 2013.

[14] A. Marinoni, P. Savazzi, and R. D. Wesel, "Protograph-based q-ary LDPC codes for higher-order modulation.," *IEEE Intl. Symp. on Turbo Codes and Iterative Information Processing*, Sep. 2010.